Electronic Supplementary Material (ESI) for Journal of Materials Chemistry C.
This journal is © The Royal Society of Chemistry 2019

Order-disorder transformation of intercalated cations triggering huge negative thermal expansion, switchable dielectrics and ion conduction near room temperature in a 2D vanadium oxide hybrid

Zhi-Yuan Yao,[a] Yin Qian,[a] Qiu Ren,[a] Guo-Qin Zhang,[a] Jin Zhang,[a] Wen-Long Liu,*[b] Hong-Bin Luo,[a] Xiao-Ming Ren*[a,c,d]

[a]State Key Laboratory of Materials-Oriented Chemical Engineering and College of Chemistry and Molecular Engineering, Nanjing Tech University, Nanjing 211816, P. R. China

[b]College of Chemistry and Chemical Engineering, Yangzhou University, Yangzhou 225002, P. R. China

[c]College of Materials Science and Engineering, Nanjing Tech University, Nanjing 211816, P. R. China

[d]State Key Laboratory of Coordination Chemistry, Nanjing University, Nanjing 210023, P. R. China

Email:

njulwl@163.com (WLL)

xmren@njtech.edu.cn (XMR)

Contents

Figure S1: (a, b) Experimental and simulated PXRD patterns of **1** at ambient temperature (c) simulated PXRD pattern of **1** with diffraction indices. The diffractions appeared at 2θ = 10.46, 11.05, 11.47, 11.68 and 22.68° corresponds to the diffractions of (0 1 1), (1 0 0), (0 0 2), (1 0 -1) and (2 0 0), respectively. These diffractions should disappear in the PXRD pattern of **1** according to the systematic absence law of the crystal's X-ray diffraction if the crystal does not have any defect. We observed these diffractions because of the existence of defects in the crystal. In addition, the diffractions at 2θ ~ 15° are not observed, which is probably due to the orientation of crystals in the measurement process.

Figure S2: (a) Four different coordination polyhedra in **1** at 293 K where the symmetric codes: #3 = 1-x, -y, 1-z; #5 = 1-x, 1-y, 1-z; #6 = -x, 1-y, 1-z; #7 = -x, -y, 1-z (b) packing diagram viewed along b-axis, which shows layered structure and the layers are parallel to the crystallographic plane of (0 0 1) and (c) packing diagram viewed along c-axis at 293 K in LTP.

Figure S3: Packing diagrams viewed along (a) b-axis, which shows layered structure and the layers are parallel to the crystallographic plane of (0 0 1) and (b) c-axis at 373 K in HTP.

Figure S4: The valence of vanadium ions in the coordination square pyramids and tetrahedra (there are four different vanadium ions, labeled as V1-V4 in LTP; two different vanadium ions, labeled as V1 and V2 in HTP).

Figure S5: χ_m-T plot of **1**, in which χ_m represents the molar magnetic susceptibility with two V^{4+} and two V^{5+} ions per formula unit $C_3H_{12}O_{10}N_2V_4$.

Figure S6: Plots of lattice parameters (*a*, *b*, *c* and *V*) as a function of temperature in the form of natural logarithm for **1**. Herein, the linear fitting was performed for *a*, *b* and *c* in the temperature ranges of 90-250 K; for *V* in the temperature ranges of 90-250 K and 293-330 K, respectively. The coefficient of thermal expansion of lattice is given by

$$\alpha_L = \frac{1}{L}\left(\frac{\partial L}{\partial T}\right)_p = \left(\frac{\partial ln(L)}{\partial T}\right)_p$$

In which L represents the lattice parameters *a*, *b*, *c* and *V*. In the plot of ln*L* vs. T, the slope $\frac{1}{L}(\frac{\partial L}{\partial T})_p = (\frac{\partial ln(L)}{\partial T})_p$ corresponds to the lattice coefficient of thermal expansion.

Figure S7: Thermal ellipsoid plots of VO_5 and VO_4 units, which are set at 50% probability level, at (a) 250 (b) 293 (c) 300 (d) 313 (e) 330 (f) 343 and (g) 373 K. In (a-d), O3, O5, O7 and O10 are the O atoms of V=O bonds in vanadyl groups; and in (e-g), O1 and O5 are the O atoms of V=O bonds in vanadyl groups.

Figure S8: Impedance plots at selected temperatures in the range of 223-493 K.

Figure S9: (a) Plots of ε′ vs T at the selected frequencies (b, c) plots of modulus imaginary part versus temperature in the frequency range of 1.0-1.0×10^7 Hz (d) plot of ln(f_{max}) vs. 1000/T for the dielectric relaxation occurring in the low temperature region in **1**, where the solid squares represent the experimental data and the red line is fitted curve using the Arrhenius equation of ln(f_{max}) = ln(f_0)-E_a/(k_BT). In Arrhenius equation, f_{max} is the frequency at the maximum of a dielectric relaxation peak, f_0 is pre-exponential factor, E_a is the dielectric relaxation activation energy. The best fit was performed in the temperature range of 193-313 K to the E_a = 0.4 eV.

Table S1: V-O Bond lengths (Å) in **1** in the temperature ranges of 90-313 K in LTP.

Table S2: V-O Bond lengths (Å) in **1** in the temperature ranges of 330-373 K in HTP.

Table S3: The selected bond lengths and bond valence sum (BVS) calculated of V at 90K and 330K

Table S4: Volumetric thermal expansion coefficient in typical NTE materials.

Table S5: Typical V-O and V=O bond distances (Å) in VO_4 (coordination tetrahedron) and VO_5 (coordination square pyramid) in the literatures.

Table S6: Crystallographic data and structural refinements for **1** in LTP.

Table S7: Crystallographic data and structural refinements for **1** in HTP.

Table S8: H-bond parameters in N-H…O of **1** in LTP at 90 K to 300K.

Table S9: H-bond parameters in N-H…O of **1** in HTP at 343 K.

Table S10: H-bond parameters in N-H…O of **1** in HTP at 373 K.

References

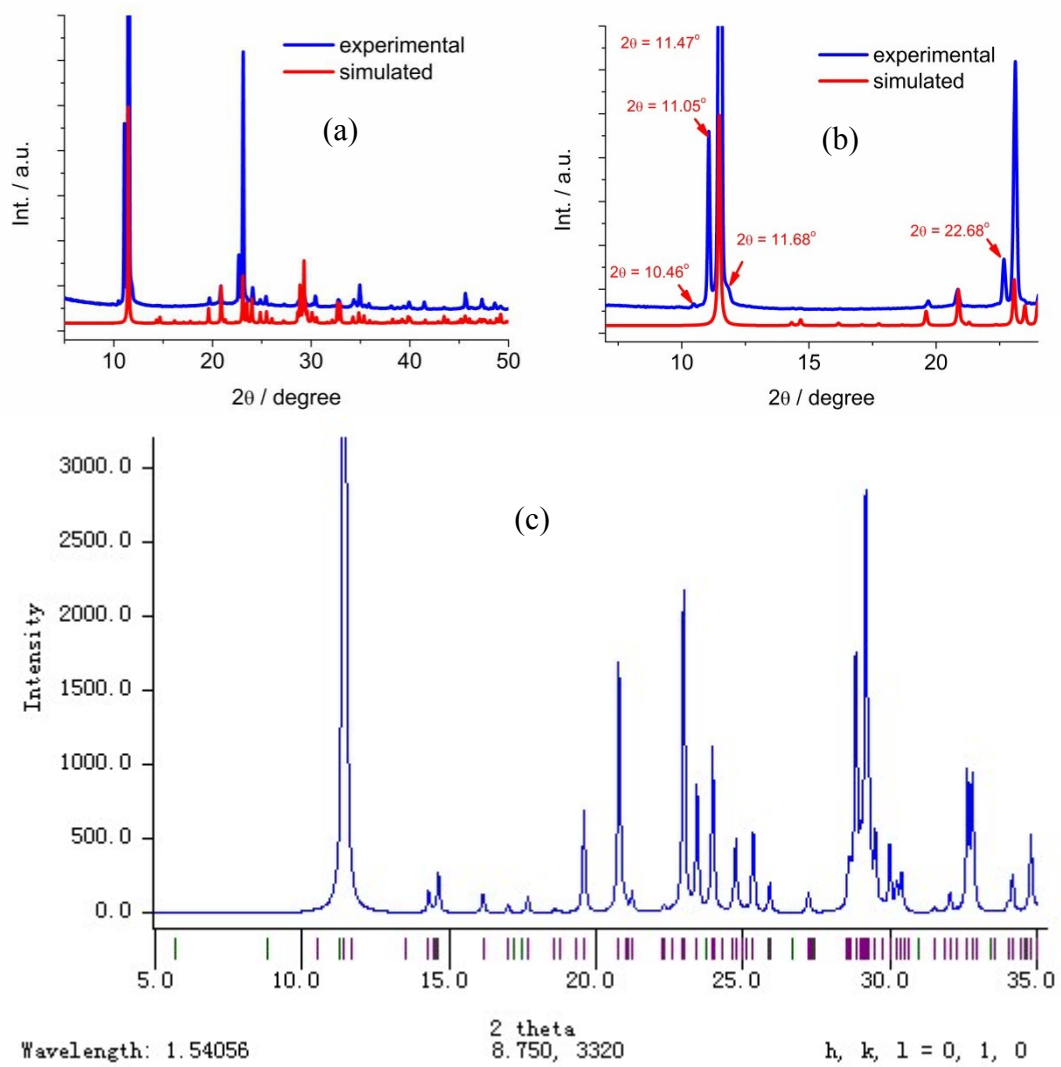

Figure S1: (a, b) Experimental and simulated PXRD patterns of **1** at ambient temperature (c) simulated PXRD pattern of **1** with diffraction indices. The diffractions appeared at 2θ = 10.46, 11.05, 11.47, 11.68 and 22.68° corresponds to the diffractions of (0 1 1), (1 0 0), (0 0 2), (1 0 -1) and (2 0 0), respectively. These diffractions should disappear in the PXRD pattern of **1** according to the systematic absence law of the crystal's X-ray diffraction if the crystal does not have any defect. We observed these diffractions because of the existence of defects in the crystal. In addition, the diffractions at 2θ ~ 15° are not observed, which is probably due to the orientation of crystals in the measurement process.

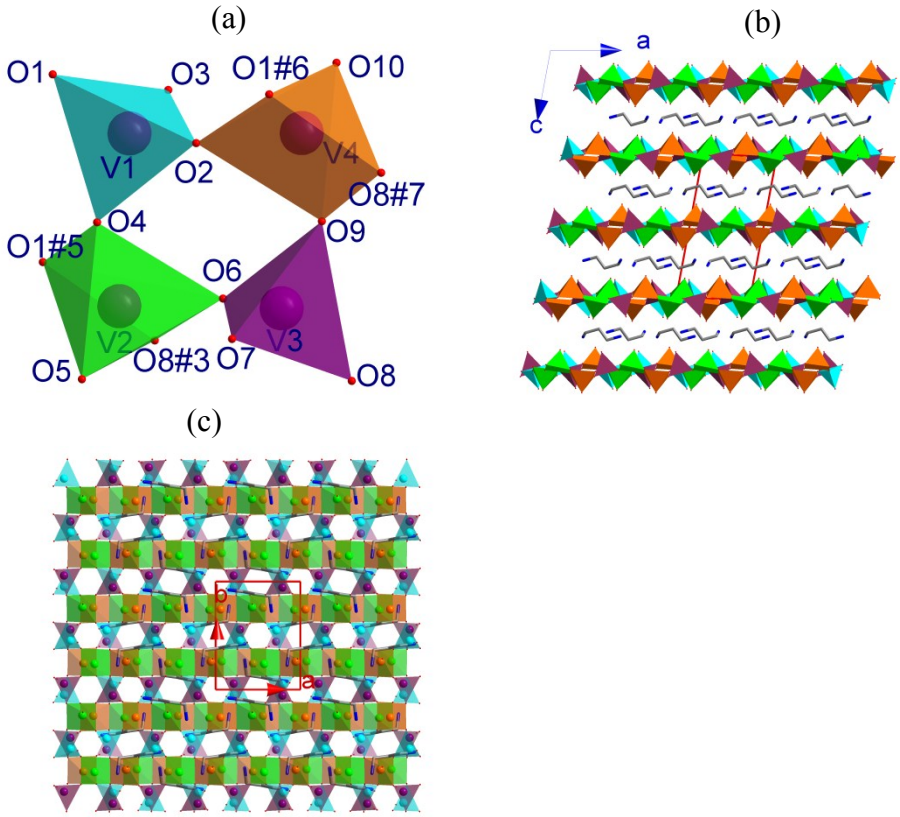

Figure S2: (a) Four different coordination polyhedra in **1** at 293 K where the symmetric codes: #3 = 1-x, -y, 1-z; #5 = 1-x, 1-y, 1-z; #6 = -x, 1-y, 1-z; #7 = -x, -y, 1-z (b) packing diagram viewed along b-axis, which shows layered structure and the layers are parallel to the crystallographic plane of (0 0 1) and (c) packing diagram viewed along c-axis at 293 K in LTP.

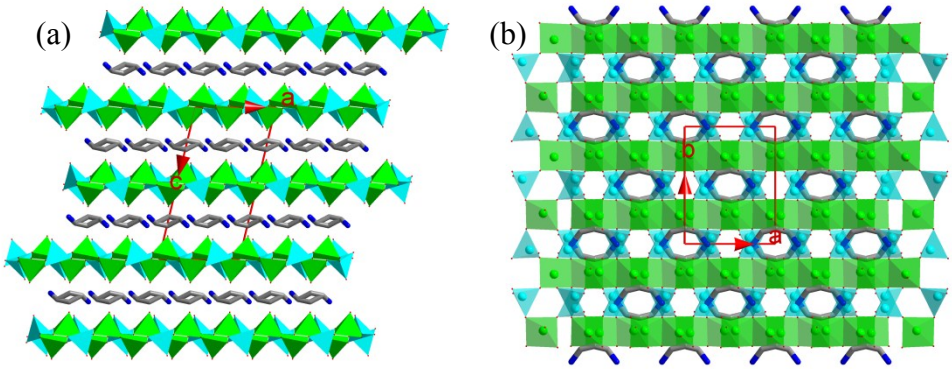

Figure S3: Packing diagrams viewed along (a) b-axis, which shows layered structure and the layers are parallel to the crystallographic plane of (0 0 1) and (b) c-axis at 373 K in HTP.

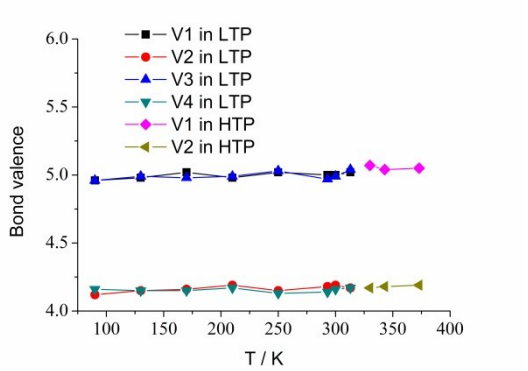

Figure S4: The valence of vanadium ions in the coordination square pyramids and tetrahedra (there are four different vanadium ions, labeled as V1-V4 in LTP; two different vanadium ions, labeled as V1 and V2 in HTP).

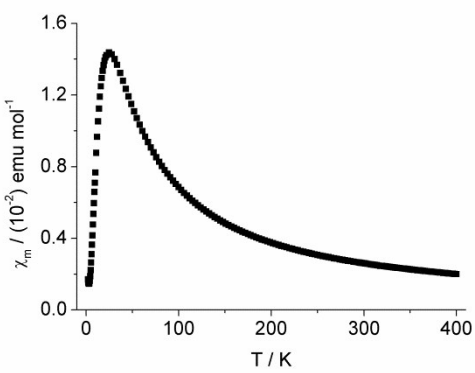

Figure S5: χ_m-T plot of **1**, in which χ_m represents the molar magnetic susceptibility with two V^{4+} and two V^{5+} ions per formula unit $C_3H_{12}O_{10}N_2V_4$.

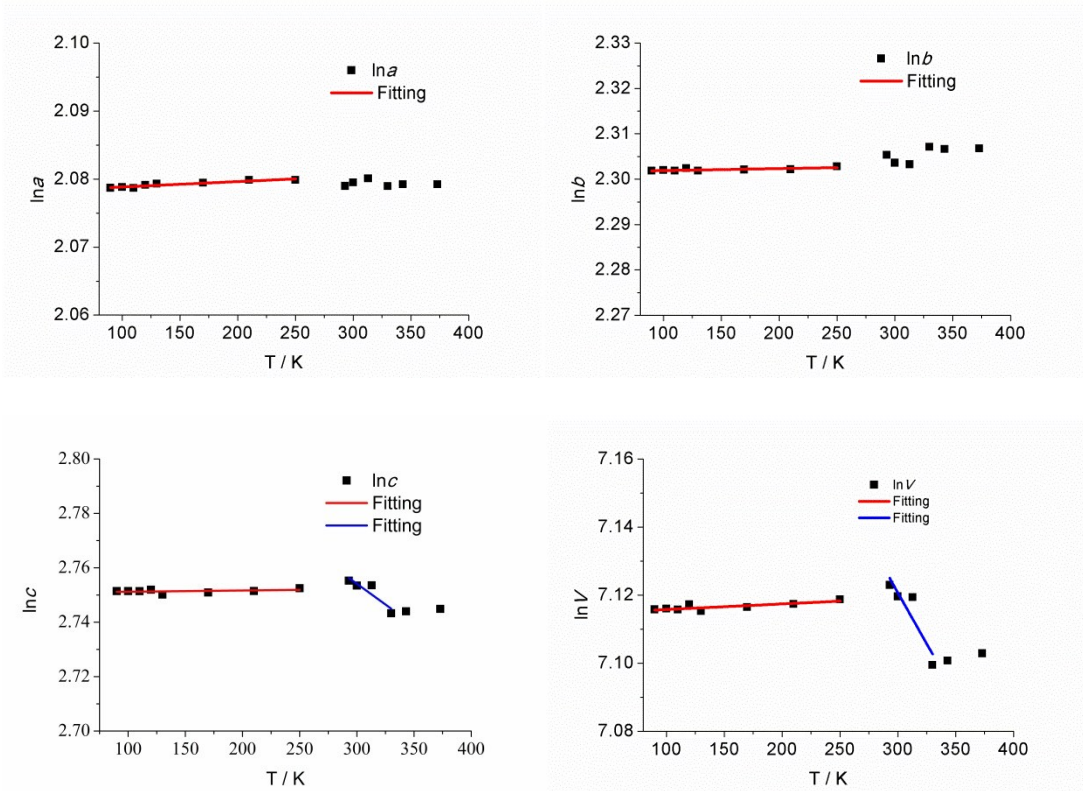

Figure S6: Plots of lattice parameters (a, b, c and V) as a function of temperature in the form of natural logarithm for **1**. Herein, the linear fitting was performed for a, b and c in the temperature ranges of 90-250 K; for V in the temperature ranges of 90-250 K and 293-330 K, respectively. The coefficient of thermal expansion of lattice is given by

$$\alpha_L = \frac{1}{L}(\frac{\partial L}{\partial T})_p$$

In which L represents the lattice parameters a, b, c and V. In the plot of ln$L$ vs. T, the slope $\frac{1}{L}(\frac{\partial L}{\partial T})_p$ corresponds to the lattice coefficient of thermal expansion.

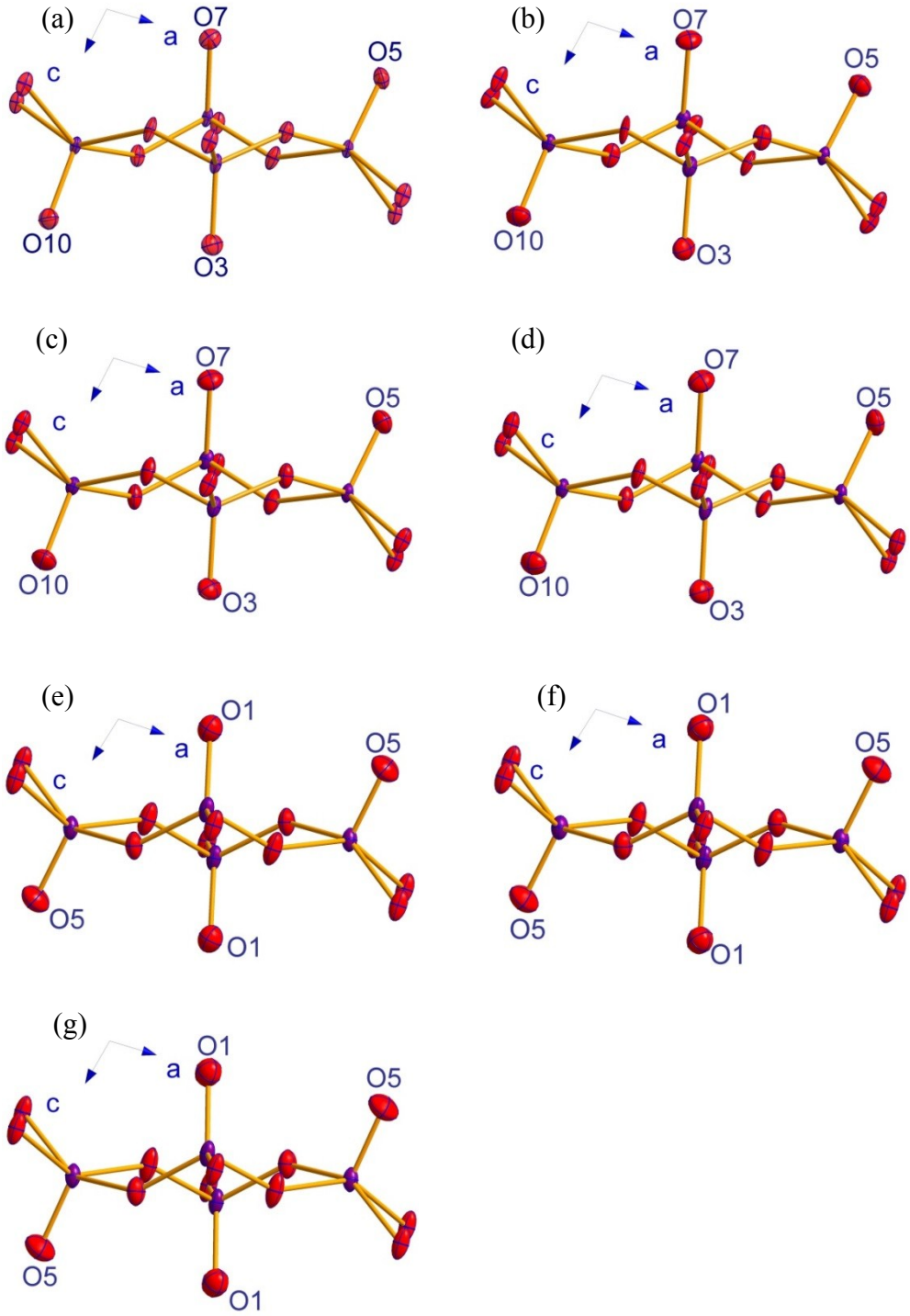

Figure S7: Thermal ellipsoid plots of VO_5 and VO_4 units, which are set at 50% probability level, at (a) 250 (b) 293 (c) 300 (d) 313 (e) 330 (f) 343 and (g) 373 K. In (a-d), O3, O5, O7 and O10 are the O atoms of V=O bonds in vanadyl groups; and in (e-g), O1 and O5 are the O atoms of V=O bonds in vanadyl groups.

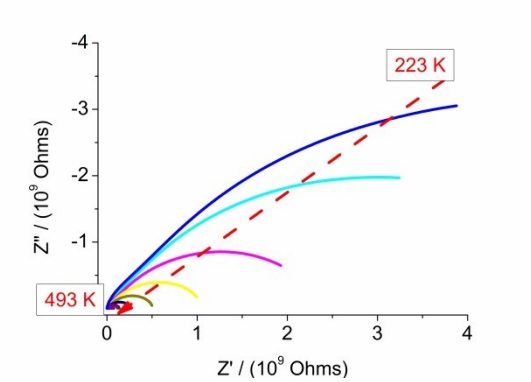

Figure S8: Impedance plots at selected temperatures in the range of 223-493 K.

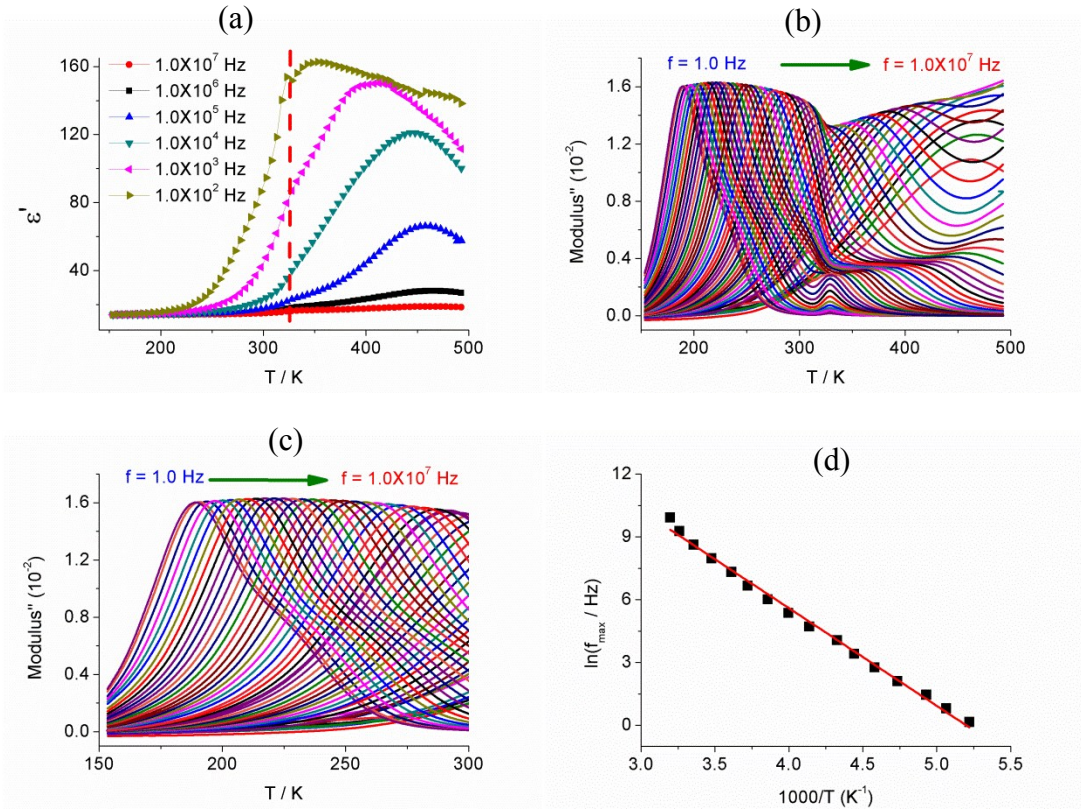

Figure S9: (a) Plots of ε′ vs T at the selected frequencies (b, c) plots of modulus imaginary part versus temperature in the frequency range of 1.0-1.0×10^7 Hz (d) plot of ln(f_{max}) vs. 1000/T for the dielectric relaxation occurring in the low temperature region in **1**, where the solid squares represent the experimental data and the red line is fitted curve using the Arrhenius equation of ln(f_{max}) = ln(f_0)-E_a/(k_BT). In Arrhenius equation, f_{max} is the frequency at the maximum of a dielectric relaxation peak, f_0 is pre-exponential factor, E_a is the dielectric relaxation activation energy. The best fit

was performed in the temperature range of 193-313 K to the E_a = 0.4 eV.

Table S1: V-O Bond lengths (Å) in **1** in the temperature ranges of 90-313 K in LTP

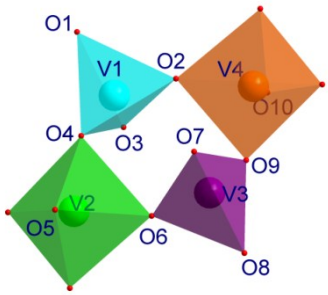

Temp. / K	90	100	110	120	130
V1-O3	1.653(4)	1.655(4)	1.654(4)	1.652(4)	1.655(4)
V1-O2	1.708(4)	1.705(4)	1.704(4)	1.712(4)	1.704(4)
V1-O4	1.722(4)	1.721(4)	1.720(4)	1.723(4)	1.717(4)
V1-O1	1.831(4)	1.839(4)	1.836(4)	1.833(4)	1.835(4)
V2-O5	1.619(4)	1.613(4)	1.621(4)	1.615(4)	1.613(4)
V2-O6	1.923(4)	1.919(4)	1.917(4)	1.925(4)	1.920(4)
V2-O4	1.936(4)	1.934(4)	1.934(4)	1.936(4)	1.934(4)
V2-O1#1	1.976(4)	1.975(4)	1.976(4)	1.980(4)	1.975(4)
V2-O8#2	1.968(4)	1.970(4)	1.966(4)	1.966(4)	1.968(4)
V3-O7	1.659(4)	1.656(4)	1.652(4)	1.653(4)	1.657(4)
V3-O6	1.697(4)	1.701(4)	1.701(4)	1.696(4)	1.697(4)
V3-O9	1.719(4)	1.717(4)	1.719(4)	1.718(4)	1.714(4)
V3-O8	1.842(4)	1.837(4)	1.840(4)	1.840(4)	1.840(4)
V4-O10	1.607(4)	1.609(4)	1.608(4)	1.609(4)	1.610(4)
V4-O2	1.928(4)	1.928(4)	1.932(4)	1.926(4)	1.926(4)
V4-O9	1.936(4)	1.937(4)	1.934(4)	1.933(4)	1.936(4)
V4-O1#3	1.972(4)	1.966(4)	1.967(4)	1.971(3)	1.967(4)
V4-O8#4	1.972(4)	1.975(4)	1.974(4)	1.977(4)	1.975(4)

Symmetry codes: #1 = 1-x, 1-y, 1-z, #2 =1-x, -y, 1-z, #3 = -x, 1-y, 1-z, #4 = -x, -y, 1-z

Continue

Temp. / K	170	210	250	293	300
V1-O3	1.649(4)	1.648(4)	1.649(4)	1.652(4)	1.653(3)
V1-O2	1.700(4)	1.706(4)	1.701(4)	1.699(4)	1.699(3)
V1-O4	1.720(4)	1.719(4)	1.716(4)	1.715(4)	1.719(3)
V1-O1	1.830(4)	1.839(4)	1.833(4)	1.839(4)	1.835(3)
V2-O5	1.612(4)	1.606(4)	1.613(4)	1.607(4)	1.609(3)
V2-O6	1.916(4)	1.918(4)	1.915(4)	1.910(4)	1.909(3)
V2-O4	1.933(4)	1.934(4)	1.937(4)	1.934(4)	1.931(3)
V2-O1#1	1.978(4)	1.973(4)	1.976(4)	1.979(3)	1.973(3)
V2-O8#2	1.970(4)	1.970(4)	1.968(4)	1.973(4)	1.972(3)
V3-O7	1.656(4)	1.652(4)	1.652(4)	1.657(4)	1.654(3)
V3-O6	1.702(4)	1.701(4)	1.698(4)	1.708(4)	1.703(3)
V3-O9	1.715(4)	1.717(4)	1.710(4)	1.709(4)	1.714(3)
V3-O8	1.840(3)	1.839(4)	1.837(3)	1.841(3)	1.838(3)
V4-O10	1.607(4)	1.610(4)	1.608(4)	1.605(4)	1.608(3)
V4-O2	1.931(4)	1.927(4)	1.931(4)	1.931(4)	1.927(3)
V4-O9	1.936(4)	1.928(4)	1.938(4)	1.938(4)	1.929(3)
V4-O1#3	1.970(3)	1.966(4)	1.972(4)	1.973(3)	1.974(3)
V4-O8#4	1.973(4)	1.973(4)	1.978(4)	1.982(4)	1.975(3)

Symmetry codes: #1 = 1-x, 1-y, 1-z, #2 =1-x, -y, 1-z, #3 = -x, 1-y, 1-z, #4 = -x, -y, 1-z

Continue

Temp. / K	313
V1-O3	1.648(4)
V1-O2	1.701(4)
V1-O4	1.715(4)
V1-O1	1.838(4)
V2-O5	1.607(4)
V2-O6	1.915(4)
V2-O4	1.940(4)
V2-O1#1	1.976(4)
V2-O8#2	1.972(4)
V3-O7	1.647(4)
V3-O6	1.702(4)
V3-O9	1.710(4)
V3-O8	1.837(3)
V4-O10	1.606(4)
V4-O2	1.928(4)
V4-O9	1.937(4)
V4-O1#3	1.967(4)
V4-O8#4	1.973(4)

Symmetry codes: #1 = 1-x, 1-y, 1-z, #2 =1-x, -y, 1-z, #3 = -x, 1-y, 1-z, #4 = -x, -y, 1-z

Table S2: V-O Bond lengths (Å) in **1** in the temperature ranges of 330-373 K in HTP

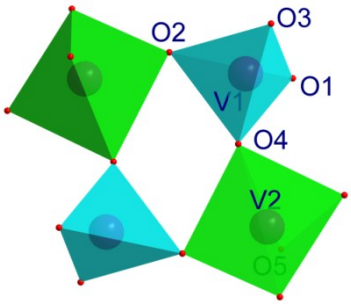

T = 330k		T = 343K		T = 373K	
V1-O1	1.632(4)	V1-O1	1.635(4)	V1-O1	1.634(4)
V1-O4	1.694(3)	V1-O4	1.696(3)	V1-O4	1.696(3)
V1-O3	1.728(3)	V1-O3	1.732(3)	V1-O3	1.730(3)
V1-O2	1.837(3)	V1-O2	1.835(3)	V1-O2	1.833(3)
V2-O5	1.602(4)	V2-O5	1.602(4)	V2-O5	1.600(4)
V2-O4	1.924(3)	V2-O4	1.921(3)	V2-O4	1.922(3)
V2-O3#1	1.945(3)	V2-O3#1	1.942(3)	V2-O3#1	1.940(3)
V2-O2#2	1.971(3)	V2-O2#2	1.974(3)	V2-O2#2	1.973(3)
V2-O2#3	1.975(3)	V2-O2#3	1.971(3)	V2-O2#3	1.974(3)
Symmetry codes: #1 = -x+1.5, -y+1.5, 1-z, #2 = x-0.5, y+0.5, z, #3 = 1-x, 1-y, 1-z		Symmetry codes: #1 = -x+1.5, -y+1.5, 1-z, #2 = -x+1, -y+1, -z+1, #3 = x-0.5, y+1.5, z		Symmetry codes: #1 =-x+1.5, -y+1.5, -z+1, #2 = -x+1, -y+1, -z+1, #3 = x-0.5, y+0.5, z	

Table S3: The selected bond lengths and bond valence sum (BVS) calculated of V at 90K and 330K

T/K	Space group	V atom	V-O bond	Distance r /Å	bond-valence parameter r_0	Valence state (s value)
90	$P2_1/n$	V_1	V1-O3	1.653(4)	1.803	4.96
			V1-O2	1.708(4)		
			V1-O4	1.722(4)		
			V1-O1	1.831(4)		
		V_2	V2-O5	1.619(4)	1.784	4.12
			V2-O6	1.923(4)		
			V2-O4	1.936(4)		
			V2-O1#1	1.976(4)		
			V2-O8#2	1.968(4)		
		V_3	V3-O7	1.659(4)	1.803	4.96
			V3-O6	1.697(4)		
			V3-O9	1.719(4)		
			V3-O8	1.842(4)		
		V_4	V4-O10	1.607(4)	1.784	4.16
			V4-O2	1.928(4)		
			V4-O9	1.936(4)		
			V4-O1#3	1.972(4)		
			V4-O8#4	1.972(4)		
Symmetry codes: #1 = 1-x, 1-y, 1-z, #2 =1-x, -y, 1-z, #3 = -x, 1-y, 1-z, #4 = -x, -y, 1-z						
330	*C2/c*	V_1	V1-O1	1.632(4)	1.803	5.07
			V1-O4	1.694(3)		
			V1-O3	1.728(3)		
			V1-O2	1.837(3)		
		V_2	V2-O5	1.602(4)	1.784	4.17
			V2-O4	1.924(3)		
			V2-O3#1	1.945(3)		
			V2-O2#2	1.971(3)		
			V2-O2#3	1.975(3)		
Symmetry codes: #1 = -x+1.5, -y+1.5, 1-z, #2 = x-0.5, y+0.5, z, #3 = 1-x, 1-y, 1-z						

The relationship between the bond length (r) and the bond valence (s) is described below,

$$s = exp^{r_0}\left(\frac{r_0 - r}{B}\right)$$

where B are empirically determined parameter[1] with the value of 0.37.

Table S4: Volumetric thermal expansion coefficient in typical NTE materials

Compound	β_V (10^{-6} K^{-1})	Temperature range	Ref.
$\{[FeTp(CN)_3]_2Co(Bib)_2\}\cdot 5H_2O$	-489	300-350 K	2
$Yb_8Ge_3Sb_5$	-1550	5–15 K	3
$[C_3H_{12}N_2][V_4O_{10}]$	-600	293-330 K	This work
$Mn_{0.98}CoGe$	-423	309–399K	4
$Bi_{0.95}La_{0.05}NiO_3$	-413	300–370K	5
$LaCu_3Fe_4O_{12}$	-199	373–423K	6
$Cd(CN)_2$	-61.2	150-375K	7
$AlPO_4$-17	-35.1	18–300 K	8
MOF-C22	-33.15	0–600K	9
ZrW_2O_8	-27.3	0.3–1050 K	10
$GaFe(CN)_6$	-11.85	100–475 K	11
ScF_3	-9.3	300–900 K	12
ITQ-4	-6.6~-11.1	95–510 K	13
$FeCo(CN)_6$	-4.41	4.2–300 K	14
$NiPt(CN)_6$	-3.06	100–330K	15
CHA	-1.5～-50.1	293–873 K	13
$PbTiO_3$	-1.41	293–623 K	16
$Zr_{0.4}Sn_{0.6}Mo_2O_8$	-0.18	12–600 K	17

Table S5: Typical V-O and V=O bond distances (Å) in VO_4 (coordination tetrahedron) and VO_5 (coordination square pyramid) in the literatures

Compound	Polyhedron	V-O / Å	V=O / Å	Ref.
$(NH_4)_2[VO_2]_2[TeO_4(OH)_2]$	VO_5 (SP)*	1.941(2)-2.052(2)	1.603(2)-1.649(2)	18
$\{Ni(phen)_3\}_2[V_{14}Sb_8O_{42}]\cdot phen\cdot 12H_2O$	VO_5 (SP)	1.921(4)-2.002(4)	1.596(5)-1.615(4)	19
$NaKV_4O_9\cdot 2H_2O$	VO_5 (SP)	1.931(3)-2.033(2)	1.609(3)-1.611(3)	20
$[C_6H_{17}N_3]_4[Sb_4V_{16}O_{42}]\cdot 2H_2O$	VO_5 (SP)	1.908(5)-2.029(4)	1.600(5)-1.640(4)	21
$[NH_4]_4[Sb_8V_{14}O_{42}]\cdot 2H_2O$	VO_5 (SP)	1.931(5)-1.990(5)	1.588(6)-1.618(6)	21
$K_2Mn_3(VO_4)_2(CO_3)$	VO_4 (T)**	1.688(2)-1.732(1)	-	22
$BaAg_2Cu[VO_4]_2$	VO_4 (T)	1.713-1.757	1.674-1.681	23
$K_4Te_3V_6O_{24}$	VO_4 (T)	1.822(2)-1.824(2)	1.623(2)-1.644(2)	24
$LiCdVO_4$	VO_4 (T)	1.746(2)	1.681(2)	25
$Co(Hdpa)_2V_4O_{12}$	VO_4 (T)	1.781(4)-1.847(8)	1.613(9)-1.635(5)	26
$Ni(Hdpa)_2V_4O_{12}$	VO_4 (T)	1.784(3)-1.857(5)	1.625(16)-1.708(18)	26
$(C_3H_{12}N_2)[V_4O_{10}]$ in this work	VO_5 (SP)	1.923(4)-1.976(4)	1.607(4)-1.619(4)	90K#
$(C_3H_{12}N_2)[V_4O_{10}]$ in this work	VO_4 (T)	1.697(4)-1.842(4)	1.653(4)-1.659(4)	90K
$(C_3H_{12}N_2)[V_4O_{10}]$ in this work	VO_5 (SP)	1.919(4)-1.975(4)	1.609(4)-1.613(4)	100K
$(C_3H_{12}N_2)[V_4O_{10}]$ in this work	VO_4 (T)	1.701(4)-1.839(4)	1.655(4)-1.656(4)	100K
$(C_3H_{12}N_2)[V_4O_{10}]$ in this work	VO_5 (SP)	1.917(4)-1.976(4)	1.608(4)-1.621(4)	110K
$(C_3H_{12}N_2)[V_4O_{10}]$ in this work	VO_4 (T)	1.701(4)-1.840(4)	1.652(4)-1.654(4)	110K
$(C_3H_{12}N_2)[V_4O_{10}]$ in this work	VO_5 (SP)	1.925(4)-1.980(4)	1.609(4)-1.615(4)	120K
$(C_3H_{12}N_2)[V_4O_{10}]$ in this work	VO_4 (T)	1.696(4)-1.840(4)	1.652(4)-1.653(4)	120K
$(C_3H_{12}N_2)[V_4O_{10}]$ in this work	VO_5 (SP)	1.920(4)-1.975(4)	1.610(4)-1.613(4)	130K
$(C_3H_{12}N_2)[V_4O_{10}]$ in this work	VO_4 (T)	1.697(4)-1.840(4)	1.655(4)-1.657(4)	130K
$(C_3H_{12}N_2)[V_4O_{10}]$ in this work	VO_5 (SP)	1.916(4)-1.978(4)	1.607(4)-1.612(4)	170K
$(C_3H_{12}N_2)[V_4O_{10}]$ in this work	VO_4 (T)	1.700(4)-1.840(3)	1.649(4)-1.656(4)	170K
$(C_3H_{12}N_2)[V_4O_{10}]$ in this work	VO_5 (SP)	1.918(4)-1.973(4)	1.606(4)-1.610(4)	210K
$(C_3H_{12}N_2)[V_4O_{10}]$ in this work	VO_4 (T)	1.701(4)-1.839(4)	1.648(4)-1.652(4)	210K
$(C_3H_{12}N_2)[V_4O_{10}]$ in this work	VO_5 (SP)	1.915(4)-1.978(4)	1.608(4)-1.613(4)	250K
$(C_3H_{12}N_2)[V_4O_{10}]$ in this work	VO_4 (T)	1.698(4)-1.837(3)	1.649(4)-1.652(4)	250K
$(C_3H_{12}N_2)[V_4O_{10}]$ in this work	VO_5 (SP)	1.910(4)-1.982(4)	1.605(4)-1.607(4)	293K
$(C_3H_{12}N_2)[V_4O_{10}]$ in this work	VO_4 (T)	1.699(4)-1.841(3)	1.652(4)-1.657(4)	293K
$(C_3H_{12}N_2)[V_4O_{10}]$ in this work	VO_5 (SP)	1.909(3)-1.975(3)	1.608(3)-1.609(3)	300K
$(C_3H_{12}N_2)[V_4O_{10}]$ in this work	VO_4 (T)	1.699(3)-1.838(3)	1.653(3)-1.654(3)	300K
$(C_3H_{12}N_2)[V_4O_{10}]$ in this work	VO_5 (SP)	1.915(4)-1.976(4)	1.606(4)-1.607(4)	313K
$(C_3H_{12}N_2)[V_4O_{10}]$ in this work	VO_4 (T)	1.701(4)-1.838(4)	1.647(4)-1.648(4)	313K
$(C_3H_{12}N_2)[V_4O_{10}]$ in this work	VO_5 (SP)	1.924(3)-1.975(3)	1.602(4)	330K
$(C_3H_{12}N_2)[V_4O_{10}]$ in this work	VO_4 (T)	1.694(3)-1.837(3)	1.632(4)	330K
$(C_3H_{12}N_2)[V_4O_{10}]$ in this work	VO_5 (SP)	1.921(3)-1.974(3)	1.602(4)	343K
$(C_3H_{12}N_2)[V_4O_{10}]$ in this work	VO_4 (T)	1.696(3)-1.835(3)	1.635(4)	343K
$(C_3H_{12}N_2)[V_4O_{10}]$ in this work	VO_5 (SP)	1.922(3)-1.974(3)	1.600(4)	373K
$(C_3H_{12}N_2)[V_4O_{10}]$ in this work	VO_4 (T)	1.696(3)-1.833(3)	1.634(4)	373K

Notes:

*SP and **T represent square pyramid and tetrahedron, respectively.

represents the temperature of crystal structure data collected.

Table S5 summarized the ranges of V-O single bond and V=O double bond distances in the coordination square pyramids (VO_5) and tetrahedra (VO_4) in the literatures and in this work at the selected temperatures (90-373 K) for comparison. As marked in red color, the V-O bond lengths fall in the range of 1.909(3)-1.982(4) Å in VO_5 versus 1.694(3)-1.842(4) Å in VO_4 in this work, which are comparable to the values of 1.908(5)-2.052(2) Å in VO_5 versus 1.688(2)-1.857(5) Å in VO_4 in the literatures. The V=O bond lengths fall in the range of 1.632(4)-1.659(4) Å in VO_4 versus 1.600(4)-1.621(4) Å in VO_5 in this work, which are also comparable to the values of 1.613(9)-1.708(18) Å in VO_4 versus 1.588(6)-1.649(2) Å in VO_5 in the literatures.

Table S6: Crystallographic data and structural refinements for **1** in LTP

Temperature (K)	90K	100K	110K	120K
Formula	$C_3H_{12}O_{10}N_2V_4$	$C_3H_{12}O_{10}N_2V_4$	$C_3H_{12}O_{10}N_2V_4$	$C_3H_{12}O_{10}N_2V_4$
Formula weight	439.91	439.91	439.91	439.91
CCDC number	1906041	1906481	1906488	1906443
Wavelength (Å)	0.71073	0.71073	0.71073	0.71073
Crystal size /mm	0.024×0.218×0.244	0.024×0.218×0.244	0.024×0.218×0.244	0.024×0.218×0.244
Crystal system	monoclinic	monoclinic	monoclinic	monoclinic
Space group	$P2_1/n$	$P2_1/n$	$P2_1/n$	$P2_1/n$
a / Å	7.9940(11)	7.9950(10)	7.9939(10)	7.9974(10)
b / Å	9.9928(13)	9.9939(12)	9.9924(12)	9.9982(11)
c / Å	15.6653(18)	15.6652(16)	15.6649(16)	15.6728(16)
α/ (°)	90	90	90	90
β / (°)	100.295(5)	100.289(4)	100.285(4)	100.283(4)
γ/ (°)	90	90	90	90
V / Å^3	1231.2(3)	1231.5(2)	1231.2(2)	1233.1(2)
Z	4	4	4	4
$F(000)$	864	864	864	864
$\theta_{min,max}$/°	2.429-27.492	2.429-27.477	2.429- 27.477	2.428-27.490
GOF	1.045	1.070	1.043	1.045
R_1^a, wR_2^b [$I>2\sigma(I)$]	0.0543, 0.1117	0.0533, 0.1094	0.0536, 0.1086	0.0497, 0.1021

[a] $R_1 = \sum||F_o| - |F_c|/\sum|Fo|$. [b] $wR_2 = \{\sum[w(F_o^2 - F_c^2)^2]/\sum[w(F_o^2)^2]\}^{1/2}$

Continue

Temperature (K)	130K	170K	210K	250K
Formula	$C_3H_{12}O_{10}N_2V_4$	$C_3H_{12}O_{10}N_2V_4$	$C_3H_{12}O_{10}N_2V_4$	$C_3H_{12}O_{10}N_2V_4$
Formula weight	439.91	439.91	439.91	439.91
CCDC number	1906444	1906445	1906446	1906447
Wavelength (Å)	0.71073	0.71073	0.71073	0.71073
Crystal size /mm	0.024×0.218×0.244	0.024×0.218×0.244	0.024×0.218×0.244	0.024×0.218×0.244
Crystal system	monoclinic	monoclinic	monoclinic	monoclinic
Space group	$P2_1/n$	$P2_1/n$	$P2_1/n$	$P2_1/n$
a / Å	7.9989(10)	8.0001(10)	8.0032(9)	8.0034(10)
b / Å	9.9926(10)	9.9950(10)	9.9957(10)	10.0020(10)
c / Å	15.6451(17)	15.6570(17)	15.6656(17)	15.6819(17)
α/ (°)	90	90	90	90
β / (°)	100.219(4)	100.224(4)	100.247(5)	100.358(4)
γ/ (°)	90	90	90	90
V / Å^3	1230.7(2)	1232.1(2)	1233.2(2)	1234.9(2)
Z	4	4	4	4
$F(000)$	864	864	864	864
$\theta_{min,max}$/°	2.430-27.511	2.429-27.504	2.428-27.490	2.427-27.509
GOF	1.053	1.088	1.039	1.060
$R_1{}^a$,$wR_2{}^b$ [$I>2\sigma(I)$]	0.0523, 0.1193	0.0528, 0.1151	0.0496, 0.1114	0.0518, 0.1133

[a] $R_1 = \sum||F_o| - |F_c|/\sum|Fo|$. [b] $wR_2 = \{\sum[w(F_o^2 - F_c^2)^2]/\sum[w(F_o^2)^2]\}^{1/2}$

Continue

Temperature (K)	293K	300K
Formula	$C_3H_{12}O_{10}N_2V_4$	$C_3H_{12}O_{10}N_2V_4$
Formula weight	439.91	439.91
CCDC number	1906448	1906449
Wavelength (Å)	0.71073	0.71073
Crystal size /mm	0.024×0.218×0.244	0.024×0.218×0.244
Crystal system	monoclinic	monoclinic
Space group	$P2_1/n$	$P2_1/n$
a / Å	7.9962(5)	8.0004(5)
b / Å	10.0274(9)	10.0101(6)
c / Å	15.7253(13)	15.6969(10)
α/ (°)	90	90
β / (°)	100.402(3)	100.518(2)
γ/ (°)	90	90
V / Å^3	1240.15(17)	1235.96(13)
Z	4	4
$F(000)$	864	864
$\theta_{min,max}$/°	2.421-27.494	2.425-27.542
GOF	1.018	1.061
R_1^a,wR_2^b [$I>2\sigma(I)$]	0.0448, 0.1002	0.0421, 0.1022

Table S7: Crystallographic data and structural refinements for **1** in HTP

Temperature (K)	343K	373K
Formula	$C_3H_{12}O_{10}N_2V_4$	$C_3H_{12}O_{10}N_2V_4$
Formula weight	439.91	439.91
CCDC number	1906453	1906454
Wavelength (Å)	0.71073	0.71073
Crystal size /mm	0.024×0.218×0.244	0.024×0.218×0.244
Crystal system	monoclinic	monoclinic
Space group	*C2/c*	*C2/c*
a / Å	7.9982(8)	7.9983(10)
b / Å	10.0408(9)	10.0417(11)
c / Å	15.5492(16)	15.5626(17)
α/ (°)	90	90
β / (°)	103.764(3)	103.491(5)
γ/ (°)	90	90
V / Å³	1212.9(2)	1215.4(2)
Z	4	4
F(000)	864	864
$\theta_{min,max}$/°	3.316-27.553	3.313-27.512
GOF	1.125	1.106
R_1^a, wR_2^b $[I > 2\sigma(I)]$	0.0434, 0.0932	0.0483, 0.1040

[a] $R_1 = \sum||F_o| - |F_c|/\sum|Fo|$. [b] $wR_2 = \{\sum[w(F_o^2 - F_c^2)^2]/\sum[w(F_o^2)^2]\}^{1/2}$

Table S8: H-bond parameters in N-H…O of **1** in LTP at 90 K to 300K

Temp. / K	D…A	Distance / Å	∠D-H…A	Angle / °
90	N2…O7#3	2.829(6)	∠N2-H2A…O7#3	167.0
	N2…O3#5	2.884(6)	∠N2-H2B…O3#5	149.2
	N2…O4#1	3.071(6)	∠N2-H2B…O4#1	125.6
	N2…O5#1	3.017(6)	∠N2-H2C…O5#1	110.0
	N2…O10#4	2.906(6)	∠N2-H2C…O10#4	160.2
	N1…O3	2.755(6)	∠N1-H1A…O3	174(7)
	N1…O5#2	2.819(7)	∠N1-H1B…O5#2	157(6)
	N1…O7#1	2.838(7)	∠N1-H1C…O7#1	154(6)
100	N2…O7#3	2.840(6)	∠N2-H10…O7#3	169.5
	N2…O3#5	2.883(6)	∠N2-H11…O3#5	151.2
	N2…O4#1	3.067(6)	∠N2-H11…O4#1	124.3
	N2…O5#1	3.008(6)	∠N2-H12…O5#1	113.2
	N2…O10#4	2.908(6)	∠N2-H12…O10#4	156.9
	N1…O3	2.751(6)	∠N1-H1…O3	172.9
	N1…O5#2	2.826(6)	∠N1-H2…O5#2	164.8
	N1…O7#1	2.839(6)	∠N1-H3…O7#1	156.4
110	N2…O7#3	2.841(6)	∠N2-H2A…O7#3	170.2
	N2…O3#5	2.883(6)	∠N2-H2B…O3#5	154.3
	N2…O4#1	3.068(6)	∠N2-H2B…O4#1	122.0
	N2…O5#1	3.010(6)	∠N2-H2C…O5#1	117.0
	N2…O10#4	2.907(6)	∠N2-H2C…O10#4	153.1
	N1…O3	2.756(7)	∠N1-H1A…O3	173(6)
	N1…O5#2	2.821(7)	∠N1-H1B…O5#2	158(6)
	N1…O7#1	2.837(6)	∠N1-H1C…O7#1	156(7)
120	N2…O7#3	2.840(6)	∠N2-H2A…O7#3	170.2
	N2…O3#5	2.881(5)	∠N2-H2B…O3#5	152.9
	N2…O4#1	3.065(6)	∠N2-H2B…O4#1	123.1
	N2…O5#1	3.002(6)	∠N2-H2C…O5#1	115.1
	N2…O10#4	2.905(6)	∠N2-H2C…O10#4	154.9
	N1…O3	2.759(6)	∠N1-H1A…O3	164(7)
	N1…O5#2	2.827(7)	∠N1-H1B…O5#2	164(5)
	N1…O7#1	2.840(6)	∠N1-H1C…O7#1	152(6)
130	N2…O7#3	2.831(6)	∠N2-H2A…O7#3	168.0
	N2…O3#5	2.886(6)	∠N2-H2B…O3#5	151.2
	N2…O4#1	3.069(5)	∠N2-H2B…O4#1	124.3
	N2…O5#1	3.006(6)	∠N2-H2C…O5#1	112.5
	N2…O10#4	2.910(6)	∠N2-H1C…O10#4	157.9
	N1…O3	2.751(6)	∠N1-H1A…O3	169(6)
	N1…O5#2	2.819(6)	∠N1-H1B…O5#2	169(6)

	N1…O7#1	2.838(6)	∠N1-H1C…O7#1	161(5)
170	N2…O7#3	2.832(6)	∠N2-H10…O7#3	169.0
	N2…O3#5	2.891(6)	∠N2-H11…O3#5	152.2
	N2…O4#1	3.072(5)	∠N2-H11…O4#1	123.7
	N2…O5#1	2.999(6)	∠N2-H12…O5#1	113.5
	N2…O10#4	2.904(6)	∠N2-H12…O10#4	156.2
	N1…O3	2.766(6)	∠N1-H1…O3	167(6)
	N1…O5#2	2.819(7)	∠N1-H2…O5#2	157(5)
	N1…O7#1	2.835(6)	∠N1-H3…O7#1	162(6)
210	N2…O7#3	2.883(6)	∠N2-H2A…O7#3	168.3
	N2…O3#5	2.899(6)	∠N2-H2B…O3#5	152.0
	N2…O4#1	3.071(6)	∠N2-H2B…O4#1	124.3
	N2…O5#1	3.010(6)	∠N2-H2C…O5#1	113.8
	N2…O10#4	2.916(7)	∠N2-H2C…O10#4	156.7
	N1…O3	2.746(7)	∠N1-H1A…O3	174(7)
	N1…O5#2	2.827(7)	∠N1-H1B…O5#2	165(7)
	N1…O7#1	2.848(7)	∠N1-H1C…O7#1	151(6)
250	N2…O7#3	2.834(6)	∠N2-H10…O7#3	168.4
	N2…O3#5	2.898(6)	∠N2-H11…O3#5	152.3
	N2…O4#1	3.076(6)	∠N2-H11…O4#1	123.9
	N2…O5#1	2.998(6)	∠N2-H12…O5#1	114.4
	N2…O10#4	2.919(6)	∠N2-H12…O10#4	155.8
	N1…O3	2.757(7)	∠N1-H1…O3	169(7)
	N1…O5#2	2.814(7)	∠N1-H2…O5#2	163(7)
	N1…O7#1	2.855(7)	∠N1-H3…O7#1	162(7)
293	N2…O7#3	2.848(6)	∠N2-H10…O7#3	168.0
	N2…O3#5	2.914(6)	∠N2-H11…O3#5	152.1
	N2…O4#1	3.086(6)	∠N2-H11…O4#1	124.6
	N2…O5#1	2.999(6)	∠N2-H12…O5#1	114.0
	N2…O10#4	2.933(6)	∠N2-H12…O10#4	115.8
	N1…O3	2.761(7)	∠N1-H1…O3	162(6)
	N1…O5#2	2.829(7)	∠N1-H2…O5#2	162(6)
	N1…O7#1	2.858(7)	∠N1-H3…O7#1	159(6)
300	N2…O7#3	2.837(5)	∠N2-H10…O7#3	166.5
	N2…O3#5	2.909(5)	∠N2-H11…O3#5	150.6
	N2…O4#1	3.081(5)	∠N2-H11…O4#1	125.5
	N2…O5#1	2.998(5)	∠N2-H12…O5#1	112.2
	N2…O10#4	2.929(5)	∠N2-H12…O10#4	157.9
	N1…O3	2.748(5)	∠N1-H1…O3	167(5)
	N1…O5#2	2.831(5)	∠N1-H2…O5#2	167(5)
	N1…O7#1	2.845(5)	∠N1-H3…O7#1	160(5)
Symmetric codes: #1 = x+0.5, -y+0.5, z+0.5; #2 = x-0.5, -y+0.5, z+0.5; #3 = -x+1, -y, -z+1; #4 = 1+x, y, z; #5 = -x+1.5, y-0.5, -z+1.5				

Table S9: H-bond parameters in N-H…O of **1** in HTP at 343 K

T/K	D…A	distance/Å	∠D-H…A	angle/°
343K	N1...O1#1	2.965(7)	N1-H1A...O1#1	112.9
	N1...O3	3.008(7)	N1-H1A...O3	159.4
	N1...O1#2	2.884(7)	N1-H1B...O1#2	154.7
	N1...O5#3	2.937(8)	N1-H1C...O5#3	176.7
	N2...O5#4	2.96(3)	N2-H2A...O5#4	154.0
	N2...O1#2	2.77(2)	N2-H2B...O1#2	144.9
	N2...O1#1	2.98(2)	N2-H2C...O1#1	122.8
Symmetric codes: #1 = -x+2, -y+1, -z+1; #2 = x, -y+1, z-0.5; #3 =-x+1, -y+1, -z+1; #4 = -x+1.5, -y+1.5, -z+1				

Table S10: H-bond parameters in N-H…O of **1** in HTP at 373 K

Temp. / K	D…A	Distance / Å	∠D-H…A	Angle / °
373K	N1...O1#1	2.969(8)	N1-H1A...O1#1	111.7
	N1...O3	3.010(9)	N1-H1A...O3	163.4
	N1...O1#2	2.891(8)	N1-H1B...O1#2	154.8
	N1...O5#3	2.932(8)	N1-H1C...O5#3	172.3
	N2...O1#1	2.98(2)	N2-H2A...O1#1	126.5
	N2...O3	2.93(2)	N2-H2A...O3	140.4
	N2...O5#4	2.97(3)	N2-H2A...O5#4	115.9
	N2...O1#2	2.76(2)	N2-H2A...O1#2	109.5
	N2...O5#5	3.19(3)	N2-H2B...O5#5	152.7
Symmetric codes: #1 = -x+2, -y+1, -z+1; #2 = x, -y+1, z-0.5 ; #3 = -x+1, -y+1, -z+1 ; #4 = -x+1.5, -y+1.5, -z+1 ; #5 = x+0.5, -y+1.5 , z-0.5				

References

1. I. D. Brown and D. Altermatt, *Acta Cryst.*, 1985, **B41**, 244−247.
2. J. X. Hu, Y. Xu, Y. S. Meng, L. Zhao, S. Hayami, O. Sato and T. Liu, *Angew. Chem. Int. Ed.*, 2017, **56**, 13052−13055.
3. S. Margadonna, K. Prassides, M. Chondroudi, J. R. Salvador and M. G. Kanatzidis, *Chem. Commun.*, 2005, 5754−5756.
4. J. Lin, P. Tong, K. Zhang, H. Tong, X. Guo, C. Yang, Y. Wu, M. Wang, S. Lin, L. Chen, W. Song and Y. Sun, *Appl. Phys. Lett.*, 2016, **109**, 241903.
5. M. Azuma1, W. Chen, H. Seki, M. Czapski, S. Olga, K. Oka, M. Mizumaki, T. Watanuki, N. Ishimatsu, N. Kawamura, S. Ishiwata, M. G. Tucker, Y. Shimakawa and J. P. Attfield, *Nat. Commun.*, 2011, **2**, 347.
6. Y. W. Long, N. Hayashi, T. Saito, M. Azuma, S. Muranaka and Y. Shimakawa, *Nature*, 2009, **458**, 60−63.
7. A. L. Goodwin and C. J. Kepert, *Phys. Rev. B.*, 2005, **71**, 140301.
8. M. P. Attfield and A. Sleight, *Chem. Mater.*, 1998, **10**, 2013−2019.
9. S. S. Han and W. A. Goddard, *J. Phys. Chem. C*, 2007, **111**, 15185−15191.
10. T. A. Mary, J. S. O. Evans, T. Vogt and A. W. Sleight, *Science*, 1996, **272**, 90−92.
11. Q. Gao, N. Shi, Q. Sun, A. Sanson, R. Milazzo, A. Carnera, H. Zhu, S. H. Lapidus, Y. Ren, Q. Huang, J. Chen and X. Xing, *Inorg. Chem.*, 2018, **57**, 10918−10924.
12. L. Hu, J. Chen, L. Fan, Y. Ren, Y. Rong, Z. Pan, J. Deng, R. Yu and X. Xing, *J. Am. Chem. Soc.*, 2014, **136**, 13566−13569.
13. D. A. Woodcock, P. Lightfoot, L. A. Villaescusa, M. J. Diaz-Cabanas, M. A. Camblor and D. Engberg, *Chem. Mater.*, 1999, **11**, 2508–2514.
14. S. Margadonna, K. Prassides and A. N. Fitch, *J. Am. Chem. Soc.*, 2004, **126**, 15390–15391.
15. K. W. Chapman, P. J. Chupas and C. J. Kepert, *J. Am. Chem. Soc.*, 2006, **128**, 7009–7014.

16. Z. Ren, R. Zhao, X. Chen, M. Li, X. Li, H. Tian, Z. Zhang and G. Han, *Nat. Commun.*, 2018, **9**, 1638.
17. S. E. Tallentire, F. Child, I. Fall, L. Vella-Zarb, I. R. Evans, M. G. Tucker, D. A. Keen, C. Wilson and J. S. O. Evans, *J. Am. Chem. Soc.*, 2013, **135**, 12849–12856.
18. G. Yun, Y. Hwang, H. Yun, J. Do and A. J. Jacobson, *Inorg. Chem.*, 2010, **49**, 229−233.
19. M. Wendt, C. Nather and W. Bensch, *Chem. Eur. J.*, 2016, **22**, 7747−7751.
20. M. Cui, Z. He, N. Wang, Y. Tang, W. Guo, S. Zhang, L. Wang and H. Xiang, *Dalton Trans.*, 2016, **45**, 5234−5239.
21. R. Kiebach, C. Nather and W. Bensch, *Solid State Sciences*, 2006, **8**, 964−970.
22. O. V. Yakubovich, E. V. Yakovleva, A. N. Golovanov, A. S. Volkov, O. S. Volkova, E. A. Zvereva, O. V. Dimitrova and A. N. Vasiliev, *Inorg. Chem.*, 2013, **52**, 1538−1543.
23. A. A. Tsirlin, A. Moller, B. Lorenz, Y. Skourski and H. Rosner, *Physical Review B*, 2012, **85**, 014401.
24. T. X. Zhu, J. G. Qin and P. S. Halasyamanib, *Dalton Trans.*, 2011, **40**, 8527−8532.
25. E. Gaudin, H. B. Yahia, F. J. Zuniga, J. M. Perez-Mato and J. Darriet, *Chem. Mater.*, 2005, **17**, 2436−2447.
26. R. L. LaDuca, R. S. Rarig and J. Zubieta, *Inorg. Chem.*, 2001, **40**, 607−612.